



# Simultaneous measurements of thermal conductivity and thermal diffusivity for garnet and olivine under high pressure

Masahiro Osako<sup>a,\*</sup>, Eiji Ito<sup>b</sup>, Akira Yoneda<sup>b</sup>

<sup>a</sup> Section of Astronomy and Geophysics, National Science Museum, Hyakunin-cho 3-23-1, Shinjuku, Tokyo 169-0073, Japan

<sup>b</sup> Institute for Study of the Earth's Interior, Okayama University, Yamada 827, Misasa, Tottori 682-0193, Japan

Received 14 February 2003; received in revised form 31 October 2003; accepted 31 October 2003

## Abstract

Thermal conductivity  $\lambda$  and thermal diffusivity  $\kappa$  have been measured simultaneously for garnet ( $\text{Al}_{73}\text{Py}_{25}\text{Gr}_1\text{Sp}_1$ ) and olivine ( $\text{Fo}_{93}\text{Fa}_7$ ) single crystals up to 8.3 GPa and 1100 K by using a pulse heating method. Anisotropy of thermal conduction is investigated along the three crystallographic axes, [1 0 0], [0 1 0], and [0 0 1] in olivine. The pressure dependence of  $\kappa$ , or  $\text{dln } \kappa/\text{d}P$ , is determined to be 0.03–0.04  $\text{GPa}^{-1}$  for the three crystallographic direction in olivine and 0.03  $\text{GPa}^{-1}$  for garnet, while  $\text{dln } \lambda/\text{d}P$  is determined to be  $\sim 0.04 \text{ GPa}^{-1}$  for olivine and 0.03  $\text{GPa}^{-1}$  for garnet. The anisotropy in thermal diffusivity or thermal conductivity of olivine is clearly observed in the present experimental range of pressure and temperature. It is likely that the anisotropy in thermal conduction would be maintained throughout the olivine stability field in the mantle down to 410 km depth. Heat capacities of olivine and garnet are calculated from the present  $\kappa$  and  $\lambda$ . Both the present heat capacities of olivine and garnet are consistent with the previously reported values within 5%. Those obtained for the three crystallographic direction in olivine are also consistent with each other within 6%. Further, the effect of basalt–eclogite transition on heat transportation is discussed based on the present results for garnet. It implies that the eclogite layer of the slab transmits thermal energy more effectively than the upper basaltic layer.

© 2004 Elsevier B.V. All rights reserved.

**Keywords:** Thermal conductivity; Olivine; Garnet; High pressure; Anisotropy; Heat capacity

## 1. Introduction

Thermal conductivity  $\lambda$  and thermal diffusivity  $\kappa$  of mantle materials are of vital importance for understanding the thermal state and the dynamics nature of the Earth's interior. Several investigations have been published on experimental measurements of  $\lambda$  and  $\kappa$  for mantle phases and rocks. Recently,  $\lambda$  and its pressure derivative for several mantle phases have also been estimated by theoretical approaches (e.g. Manga

and Jeanloz, 1997; Hofmeister, 1999; Cohen, 2000). Nevertheless, our knowledge of thermal conduction of the mantle phases is still insufficient to simulate heat transportation in the mantle, in particular under high-pressure and high-temperature conditions.

Thermal conductivity or thermal diffusivity measurements under high pressure were conducted by using cylindrical heat flow or linear heat flow. A cylindrical sample assembly has frequently been used in measurement of  $\lambda$  and  $\kappa$  under high pressure (e.g. Fujisawa et al., 1968; Beck et al., 1978; Katsura, 1995). Due to the requirement of axial symmetric heat flow, this method cannot be applied to investigate anisotropy in thermal conduction. On the other

\* Corresponding author. Tel.: +81-3-5332-7174;

fax: +81-3-3364-7104.

E-mail address: [sako@kahaku.go.jp](mailto:sako@kahaku.go.jp) (M. Osako).

hand, thermal conductivity  $\lambda$  of mantle materials were measured under high pressure by means of a one-dimensional thermal conduction experiment. Yukutake and Shimada (1978) measured thermal conductivity of stishovite and periclase up to 4 GPa in a cubic multi-anvil apparatus. Schärmeli (1982) conducted measurement on single crystal olivine up to 2.5 GPa in a piston-cylinder apparatus. It should be noted, however, that relatively large sample is required in those methods to accommodate multiple thermocouples in the sample. Therefore, they are not suitable for high-pressure phases of limited size.

A pulse method of one-dimensional sample configuration was developed by Dzhavadov (1975); he measured  $\lambda$  and  $\kappa$  simultaneously for a relatively large Teflon sample (3.5 mm in thickness and 20 mm in diameter). This method is applicable not only to measurement of material anisotropic in thermal conduction, but also to obtain information on heat capacity under high pressure. We have tried to substantially reduce the sample size so that the technique become applicable to mantle materials and high-pressure phases of limited size. We selected natural garnet and olivine as the samples of the present study. Garnet is accepted as major constituent in the upper mantle and the transition zone and is isotropic in thermal conduction. Measurement along different crystallographic direction in olivine should be a good test for anisotropy of thermal conduction.

## 2. Experimental

Fig. 1 shows the basic concept of the present experimental technique. The sample consists of three thin identical disks. An impulse heater is placed on one interface between the disks, and a thermocouple is inserted on the other interface. The thermal disturbance caused by impulse heating is monitored by the thermocouple. The temperature variation  $\Delta T$  at the position of the thermocouple is expressed as

$$\Delta T = A \sum_{n=1}^{\infty} \frac{1}{n^2} \sin \frac{n\pi}{3} \sin \frac{n\pi x}{d} \exp(-n^2 B t) \times [\exp(n^2 B \tau) - 1] : (t > \tau) \quad (1)$$

where  $t$  is time from the onset of heating,  $x$  the position measured from the end of the sample,  $d$  the total height

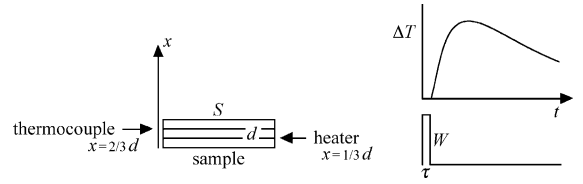


Fig. 1. A pulse heating method for measurement of thermal conductivity and thermal diffusivity after Dzhavadov (1975). Left figure shows basic configuration of the sample.  $d$  the total height of the three sample disks,  $S$  the area of the heater,  $x$  the position from the bottom of the sample (the heater is at  $x = d/3$ , and the thermocouple is at  $x = 2d/3$ ). Temperature change  $\Delta T$  caused by impulse heating with a power of  $W$  is monitored by the thermocouple (right figure), where  $\tau$  is the duration of pulse heating, and  $t$  the time from onset of the heating.

of the three sample disks, and  $\tau$  the duration of heating pulse. The quantities  $A$  and  $B$  are defined as follows:

$$A = \frac{2Wd}{\pi^2 \lambda S}, \quad B = \frac{\pi^2 \kappa}{d^2} \quad (2)$$

where  $W$  is the power of the impulse heating,  $S$  the area of the heater. Eq. (1) is derived under the boundary condition of constant temperature at the both sample ends (Dzhavadov, 1975). As the series (1) for  $\Delta T$  converges rapidly, summation up to  $n = 10$  yields very accurate value for the present experimental condition. In the present work, the parameters  $A$  and  $B$  are determined through the least square fitting of the experimental data by means of Eq. (1) up to  $n = 15$ .

We prepared natural single crystals samples of garnet and olivine for measurements of  $\kappa$  and  $\lambda$ . The garnet samples from Bahia, Brazil have a composition of 73% almandine and 25% pyrope, 1% grossular and 1% spessartine components from microprobe analysis. The garnet crystals were cut so that the surface was perpendicular to one of the crystallographic axes. The olivine samples from northern Pakistan exhibited a euhedral shape with a composition of 93% forsterite and 7% fayalite from microprobe analysis. The single crystals were cut perpendicularly to the three crystallographic axes,  $[100]$ ,  $[010]$ , and  $[001]$ . The accuracy of the cutting was within  $0.5^\circ$ . A stacking of three identical disks of the sample was used for one measurement. The dimensions of each disk were 4.3 mm in diameter and  $\sim 0.35$  mm in thickness. The three disks were polished to have same thickness within 0.002 mm.

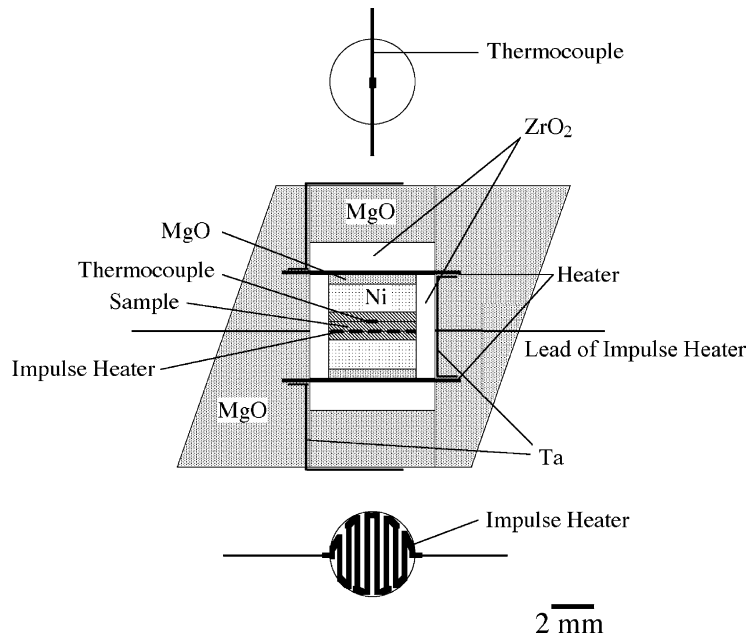


Fig. 2. Cross section of the sample assembly. Top views of thermocouple and impulse heater are also. The flat thermocouple has a thickness of 0.03 mm and a width of 0.3 mm, and the impulse heater has a thickness of 0.03 mm. Although the circuit pattern of impulse heater is shown schematically, the stripe of the impulse heater circuit is folded 20 times.

The high-pressure experiments were performed in a Kawai-type high-pressure apparatus (SHP-1000) at the Institute for Study of the Earth's Interior. A magnesia octahedron with an edge-length of 18 mm was used as a pressure medium in tungsten carbide anvils with a truncation edge length of 11 mm. Calibration of sample pressures to hydraulic oil pressure is based on the Bi I–II (2.54 GPa) and Bi III–IV (7.8 GPa) transitions. The calibration runs were made using a similar setup to that of the actual run.

Fig. 2 shows a view of the whole cell assembly used in this study. The ambient temperature of the sample consisting of three thin disks is controlled by the two plate heaters and the sample temperature was monitored by a thin flat chromel–alumel thermocouple (0.03 mm in thickness and 0.3 mm in width) inserted between the sample disks. A small heater made of nickel–chromium (3.8 mm in diameter and 0.03 mm in thickness) is placed at the other interface of the sample disks to perform impulse heating. The heater which contains photo-etched slots is effective to achieve uniform and nearly one-dimensional heating over a cross section of the sample. Transient heat

flow caused by impulse heating passes through the sample disk, and the corresponding transient signal is observed by the thermocouple as a hump on the emf of the ambient temperature. Nickel blocks contacted to the sample serve as heat sink, which is critical to keep the constant temperature boundary condition. A zirconia sleeve and blocks surrounding the assembly serve as thermal insulator for heating of the sample. The sleeve effectively restricts lateral heat flow to realize one-dimensional heat flow in the sample.

Measurements were conducted at pressures up to 8.3 GPa and at temperatures up to 1100 K. The ambient temperature is maintained by the main heater operated by a dc power supply to eliminate inductive noise. This is essential to achieve resolution of  $\sim 0.1 \mu\text{V}$  in the signal (20–100  $\mu\text{V}$ ) generated by impulse heating on the thermocouple emf.

Fig. 3 shows the schematic diagram of the measurement and a temperature profile on the storage oscilloscope. Averaging 64, 128, or 256 acquisitions was carried out for the digital records of the oscilloscope to reduce random noise. The direction of the dc impulse current was inverted one after the other on data

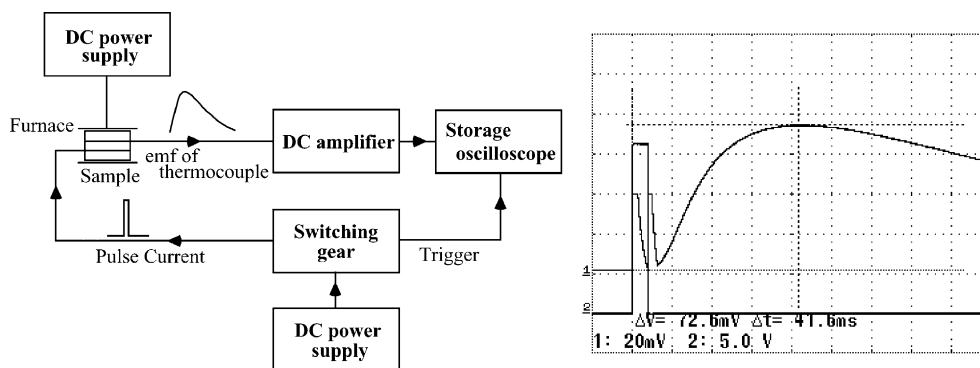


Fig. 3. Schematic diagram of the measurement (left) and a record of oscilloscope display (right) in which an input impulse and the resulted temperature profile are exhibited. One division on the vertical scale is 5 mV for the thermocouple and 5.0 V for the impulse. The horizontal scale is 10 ms per a division. Although the initial part of the temperature profile is disturbed by induction noise from the current of the impulse heater, it does not affect the measurements. The gain of the dc amplifier is 60 dB. The top height of the temperature profile corresponds to  $\sim 1$  K. The demonstrated profile yields  $\lambda = 4.15 \text{ W m}^{-1} \text{ K}^{-1}$  and  $\kappa = 1.51 \times 10^{-6} \text{ m}^2 \text{ s}^{-1}$  for impulse heating of 22.1 W input power with a duration of 3.96 ms.

acquisition to cancel the inductive noise caused by the impulse heating current.

### 3. Results and discussion

#### 3.1. Garnet

Thermal diffusivity  $\kappa$  and conductivity  $\lambda$  of garnet obtained in three runs at room temperature as functions of pressure are shown in Fig. 4. Changes in sample size during compression were corrected by using the compression data of Sato et al. (1978). The  $\kappa$  and  $\lambda$  data obtained in each run are well fitted to the linear line with respect to pressure, and are connected with thin solid lines (Fig. 4). Errors attached to each data point of  $\kappa$  (ca. 2%) are caused mainly from those associated with the uncertainty of sample thickness  $d$  and the least-square fitting procedures. On the other hand, errors of  $\lambda$  (ca. 3%) are caused by uncertainty of heating area  $S$  and power  $W$  besides by those of  $d$  and the fitting procedures. Somewhat large systematic variations in  $\kappa$  and  $\lambda$  values among the different runs are inferred to be due to slight movement of the heater and thermocouple relative to the sample disks during the initial compression. Measurements were actually carried out at slightly different temperatures of 293–297 K. The  $\kappa$  and  $\lambda$  values are adjusted to those at 293 K by using the temperature variation of

$\kappa$  in Table 3 (Osako, 1997) and the heat capacity  $C_P$  (Watanabe, 1982) at atmospheric pressure. The averaged  $\kappa$  and  $\lambda$  values after the adjustment are shown by the heavy dash-dotted lines (Fig. 4), and tabulated in Table 1. Parameters for linear fitting of  $\kappa$  and  $\lambda$

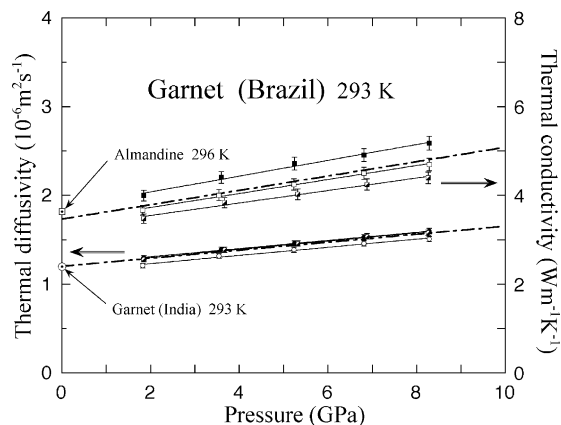


Fig. 4. Thermal diffusivity (circles) and thermal conductivity (squares) of garnet vs. pressure. Measurements were performed at slight different temperature, 293–297 K. Thermal diffusivity  $\kappa$  and thermal conductivity  $\lambda$  were obtained simultaneously for each run. The results for the three separate runs are specified by open, half-closed and closed symbols. Dash-dotted lines are averaged thermal diffusivity and thermal conductivity at 293 K. The dotted circle at zero pressure is a reference thermal diffusivity of a garnet with a similar composition measured using the Ångström method (Osako, 1997), and the dotted square indicates thermal conductivity of natural almandine (Horai, 1971).

Table 1

Thermal diffusivity  $\kappa$  and thermal conductivity  $\lambda$  of olivine and garnet at high pressures  $P$  and at various temperatures  $T$ 

	$\kappa$ and $\lambda$ at 293 K							$d\ln\kappa/dP$ $d\ln\lambda/dP$ (GPa <sup>-1</sup> )	$\kappa$ and $\lambda$ at 8.3 GPa			
	$P$ (GPa)								$T$ (K)			
	0	2	4	6	8	10	400		600	800	1000	
Olivine Fo <sub>93</sub>												
[1 0 0]	$\kappa$ (10 <sup>-6</sup> m <sup>2</sup> s <sup>-1</sup> )	[2.50 (7)]	2.67 (9)	2.86 (10)	3.05 (12)	3.27 (14)	[3.49 (16)]	0.033 (5)	2.28 (22)	1.50 (18)	1.11 (15)	0.87 (14)
	$\lambda$ (Wm K <sup>-1</sup> )	[6.61 (29)]	7.12 (35)	7.68 (42)	8.29 (49)	8.94 (57)	[9.64 (66)]	0.038 (5)	7.13 (50)	5.39 (40)	4.52 (34)	4.00 (31)
[0 1 0]	$\kappa$ (10 <sup>-6</sup> m <sup>2</sup> s <sup>-1</sup> )	[1.53 (8)]	1.66 (10)	1.80 (12)	1.95 (14)	2.11 (16)	[2.28 (20)]	0.040 (7)	1.43 (13)	0.91 (10)	0.65 (9)	0.50 (8)
	$\lambda$ (Wm K <sup>-1</sup> )	[3.95 (22)]	4.30 (26)	4.67 (30)	5.08 (35)	5.53 (41)	[6.02 (47)]	0.042 (5)	4.28 (49)	3.13 (39)	2.56 (34)	2.21 (31)
[0 0 1]	$\kappa$ (10 <sup>-6</sup> m <sup>2</sup> s <sup>-1</sup> )	[2.16 (7)]	2.32 (9)	2.48 (11)	2.66 (13)	2.85 (15)	[3.05 (18)]	0.035 (3)	2.05 (23)	1.36 (18)	1.01 (16)	0.80 (15)
	$\lambda$ (Wm K <sup>-1</sup> )	[5.91 (21)]	6.33 (24)	6.78 (27)	7.26 (31)	7.78 (35)	[8.34 (39)]	0.034 (5)	6.40 (38)	4.96 (30)	4.24 (27)	3.81 (24)
Garnet												
	$\kappa$ (10 <sup>-6</sup> m <sup>2</sup> s <sup>-1</sup> )	[1.19 (4)]	1.29 (5)	1.38 (6)	1.47 (7)	1.56 (7)	[1.66 (8)]	0.029 (1) (at 8 GPa)	1.23 (16)	0.91 (13)	0.76 (11)	0.66 (10)
	$\lambda$ (Wm K <sup>-1</sup> )	[3.48 (15)]	3.80 (18)	4.12 (20)	4.44 (23)	4.76 (25)	[5.08 (28)]	0.034 (2) (at 8 GPa)	3.77 (30)	3.19 (25)	2.89 (22)	2.72 (21)

The figures in square brackets are extrapolated values based on the present data. Pressure derivatives are also given.

Table 2

Coefficients of fitting parameters of thermal diffusivity  $\kappa$  and thermal conductivity  $\lambda$ 

Garnet				Olivine				
$\kappa = a_0 + a_1P$		$\kappa = c_0 + c_1/T$		$\kappa = b_0 \exp(b_1P)$		$\kappa = c_0 + c_1/T$		
$a_0$ (10 <sup>-6</sup> m <sup>2</sup> s <sup>-1</sup> )	$a_1$ (10 <sup>-6</sup> m <sup>2</sup> s <sup>-1</sup> GPa <sup>-1</sup> )	$c_0$ (10 <sup>-6</sup> m <sup>2</sup> s <sup>-1</sup> )	$c_1$ (10 <sup>-6</sup> m <sup>2</sup> s <sup>-1</sup> K)	$b_0$ (10 <sup>-6</sup> m <sup>2</sup> s <sup>-1</sup> )	$b_1$ (GPa <sup>-1</sup> )	$c_0$ (10 <sup>-6</sup> m <sup>2</sup> s <sup>-1</sup> )	$c_1$ (10 <sup>-6</sup> m <sup>2</sup> s <sup>-1</sup> K)	
1.19 (6)	0.046 (1)	0.29 (6)	374 (31)	[1 0 0]	2.50 (4)	0.033 (5)	-0.06 (11)	938 (46)
				[0 1 0]	1.53 (6)	0.040 (7)	-0.13 (8)	626 (45)
				[0 0 1]	2.16 (14)	0.035 (3)	-0.03 (17)	832(98)
$\lambda = A_0 + A_1P$		$\lambda = C_0 + C_1/T$		$\lambda = B_0 \exp(B_1P)$		$\lambda = C_0 + C_1/T$		
$A_0$ (W m <sup>-1</sup> K <sup>-1</sup> )	$A_1$ (W m <sup>-1</sup> K <sup>-1</sup> GPa <sup>-1</sup> )	$C_0$ (W m <sup>-1</sup> K <sup>-1</sup> )	$C_1$ (W m <sup>-1</sup> )	$B_0$ (W m <sup>-1</sup> K <sup>-1</sup> )	$B_1$ (GPa <sup>-1</sup> )	$C_0$ (W m <sup>-1</sup> K <sup>-1</sup> )	$C_1$ (W m <sup>-1</sup> )	
3.48 (33)	0.160 (26)	2.01 (8)	704 (43)	[1 0 0]	6.61 (13)	0.038 (5)	1.91 (28)	2088 (163)
				[0 1 0]	3.98 (15)	0.042 (5)	0.84 (36)	1377 (157)
				[0 0 1]	5.91 (25)	0.034 (5)	2.08 (38)	1731 (86)

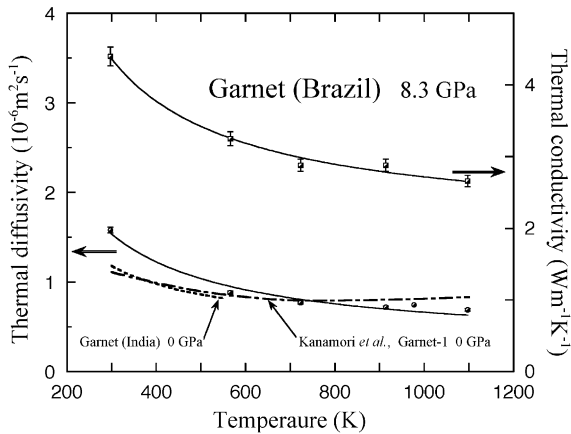


Fig. 5. Thermal diffusivity and thermal conductivity of garnet vs. temperature at 8.3 GPa. Dash-dotted and dashed lines correspond to values at 0 GPa by an Ångström method.

are listed in Table 2. The extrapolated value of  $\kappa$  to zero-pressure agrees well with that determined by the Ångström method (Osako, 1997), and the extrapolated  $\lambda$  is consistent with that by Horai (1971).

Fig. 5 shows temperature dependence of  $\kappa$  and  $\lambda$  of garnet at 8.3 GPa. Corrections for length were made using thermal expansion data (c). Data for both  $\kappa$  and  $\lambda$  are fitted to an empirical form,  $c_0 + c_1/T$ , where  $c_0$  and  $c_1$  are fitting parameters and  $T$  is absolute temperature. The values are tabulated in Table 1 and the parameters listed in Table 2. The temperature derivatives for both  $\kappa$  and  $\lambda$  diminish with increasing temperature, as observed at zero-pressure in previous studies (Kanamori et al., 1968; Osako, 1997).

### 3.2. Olivine

The  $\kappa$  and  $\lambda$  values of olivine at room temperatures are plotted against pressure in Fig. 6a and b, respectively. The changes of the sample sizes during compression were corrected using recent compression data for San Carlos olivine by Zha et al. (1998). Magnitude and sources of the errors are similar to those for garnet. Two or three high-pressure measurements were carried out for each crystallographic axis. The data are better fitted to an exponential expression with a constant pressure derivative than to the linear relation in the cases of garnet, and are connected with thin solid lines in Fig. 6a and b. Variations over the different

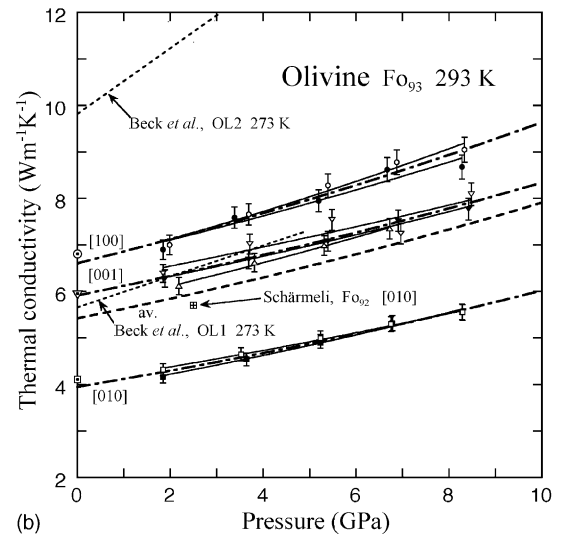
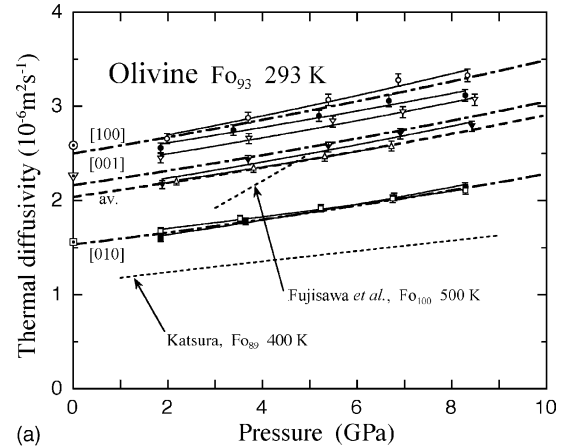


Fig. 6. (a) Thermal diffusivities  $\kappa$  of olivine vs. pressure at room temperature. Measurements were performed at slightly different temperature, 290–298 K. Symbols of circles, squares and triangles denote measurements for [100], [010] and [001] axes, respectively. Two or three runs were carried out for each crystallographic axis. Dash-dotted lines indicate adjusted data for 293 K. Dotted symbols at 0 GPa are thermal diffusivities at zero pressure are determined by the Ångström method (Osako, 1997). Heavy dashed line indicates averaged  $\kappa$  for the three axes; its pressure derivatives are close to those reported by Katsura (1995) for olivine polycrystalline aggregate but much lower than that reported by Fujisawa et al. (1968) for forsterite. (b) Thermal conductivities vs. pressure at room temperature compared with previous results. Each symbols corresponds to the same run of thermal diffusivity measurements. Dash-dotted lines show adjusted values at 293 K. Heavy dashed line indicates averaged  $\lambda$  for the three axes; thermal conductivity at zero pressure is calculated from the thermal diffusivity and heat capacity (Watanabe, 1982).

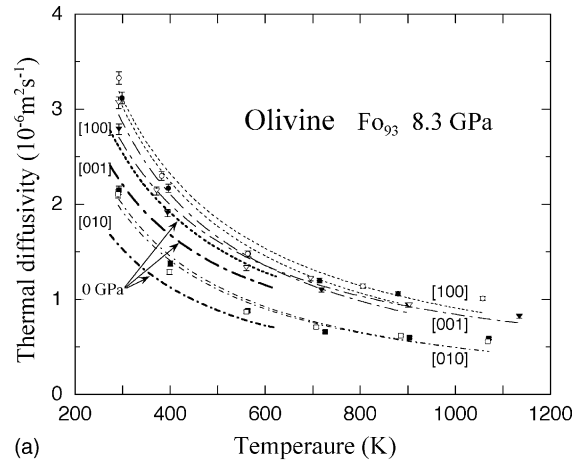
Table 3  
Coefficients of fitting parameters of thermal diffusivity  $\kappa$  of olivine (Fo<sub>93</sub>) and garnet (Py<sub>34</sub>Al<sub>57</sub>Sp<sub>1</sub>Gr<sub>8</sub>) at 0 GPa by an Ångström method (Osako, 1997)

	$\kappa = c_0 + c_1/T$	
	$c_0$ ( $10^{-6} \text{ m}^2 \text{ s}^{-1}$ )	$c_1$ ( $10^{-6} \text{ m}^2 \text{ s}^{-1} \text{ K}$ )
Garnet	0.39 (2)	236 (9)
Olivine		
[1 0 0]	0.04 (5)	747 (17)
[0 1 0]	-0.07 (2)	478 (9)
[0 0 1]	0.09 (5)	634 (19)

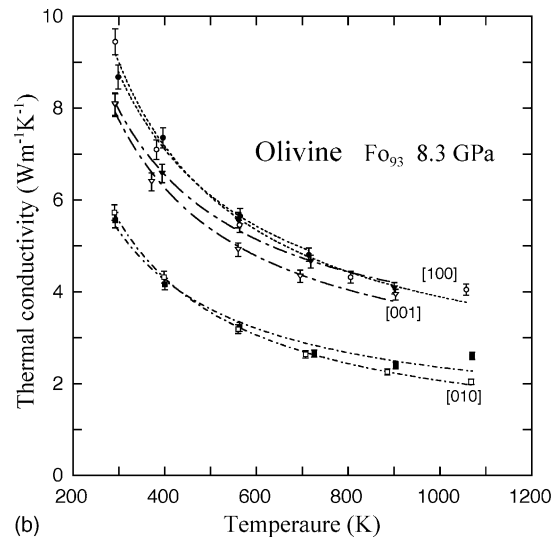
runs are inferred to be originated from similar sources as in the garnet measurement.

The data at slightly different temperatures (290–298 K) are adjusted to values corresponding to 293 K by the same procedure as in the case of garnet. The averaged value after the adjustment are shown by the heavy dash-dotted lines for each crystallographic axis for both  $\kappa$  (Fig. 6a) and  $\lambda$  (Fig. 6b) and are tabulated in Table 1. The fitting parameters are listed in Table 3. The intersections of these lines with the vertical axis give the room temperature values of  $\kappa$  and  $\lambda$  that are very close to the  $\kappa$  obtained by an Ångström method at 0 GPa by Osako (1997) in Table 3 and the  $\lambda$  calculated by the measured  $\kappa$  and heat capacity by Watanabe (1982).

The pressure dependence of  $\kappa$  in this study, 3–4% GPa<sup>-1</sup>, is close to that reported by Katsura (1995) for olivine polycrystalline aggregate, although the value of  $\kappa$  itself is significantly different, which cannot be explained by the temperature dependence and the effect of composition (Horai, 1971). Measurements of olivine by Beck et al. (1978) show dependence in  $\lambda$  of 5–6% GPa<sup>-1</sup>, although the sample orientation in their experiment is not clearly specified. A theoretical calculation (Hofmeister, 1999) predicts pressure dependence of 4% GPa<sup>-1</sup> for  $\lambda$  of olivine. On the other hand, the pressure dependence of  $\kappa$  reported by Fujisawa et al. (1968) for forsterite shows a much higher value than that in the present measurements. In their work the use of thick thermocouples compared to the diameter of samples may be responsible for the observed differences. As a result, it can be concluded that pressure dependence in  $\kappa$  or  $\lambda$  of olivine is close to 3–4% GPa<sup>-1</sup>.



(a)



(b)

Fig. 7. (a) Thermal diffusivity of olivine vs. temperature under high pressure. Symbols of circles, squares and triangles denote measurements for [100], [010] and [001] axes, respectively. Heavy lines are thermal diffusivity at zero pressure obtained by an Ångström method in Table 3 (Osako, 1997). (b) Thermal conductivity of olivine vs. temperature under high pressure. Each symbol represents a separate run for the thermal diffusivity and thermal conductivity measurements.

Temperature dependence of  $\kappa$  and  $\lambda$  of olivine at 8.3 GPa are shown in Fig. 7. Small correction of sample size due to thermal expansion (Suzuki, 1975) was made. Two runs were performed for each crystallographic axis. The results for each axis are reproducible within the magnitude of estimated errors except for those over 1000 K. Data for both  $\kappa$  and  $\lambda$  decreased

with temperature and are fitted to an empirical form,  $c_0 + c_1/T$ , where  $c_0$  and  $c_1$  are fitting parameters and  $T$  is absolute temperature. The values are tabulated in Table 1 and the parameters listed in Table 2. In both  $\kappa$  and  $\lambda$ , the values along [1 0 0] and [0 0 1] directions become close to each other with increasing temperature. However the anisotropy in thermal conduction remains rather large between [0 1 0] and either [1 0 0] or [0 0 1] directions even at 1100 K.

It is well established that olivine has a high anisotropy in thermal conductivity at zero pressure (e.g. Kobayashi, 1974, Chai et al., 1996, Osako, 1997). In addition, high-pressure measurements by Beck et al. (1978), have shown olivine remains anisotropic in thermal conductivity at pressures up to 5 GPa, and those by Schärmeli (1982) demonstrate it is also anisotropic at temperatures up to 1500 K at 2.5 GPa. The results in the present study clearly indicate the olivine remains anisotropic in an extended pressure range up to 8.3 GPa and temperatures up to 1100 K. It is highly likely, therefore, that the anisotropy in thermal conduction found in the present study would be maintained throughout the olivine stability field in the mantle down to 410 km depth.

### 3.3. Heat capacity

Heat capacity  $C$  can be obtained from  $\lambda$  and  $\kappa$ :

$$C = \frac{\lambda}{\rho\kappa} \quad (3)$$

The boundary condition of the measurement indicates that the calculated  $C$  should be a kind of average between  $C_P$  and  $C_V$ , however the small difference between  $C_P$  and  $C_V$  is negligible in this discussion. The calculated heat capacities for garnet and olivine are shown and compared with the previous

data (Watanabe, 1982) in Table 4. Heat capacities of olivine calculated for different crystal axis coincide within 6%, which support the internal consistency of the present-measurements of  $\kappa$  and  $\lambda$ . The heat capacity of olivine and garnet obtained from  $\kappa$  and  $\lambda$  agree with those observed by calorimetric measurements within 5%. Thermodynamical considerations indicate that  $dC/dP$  must be negative. The measured  $dC/dP$  for olivine are comparable with estimation from known thermodynamic parameters with one order of magnitude, although the positive  $dC/dP$  determined for garnet remains for discussion; this may be caused by somewhat large systematic errors in  $\lambda$  as seen in Fig. 4. Thus, considering difficulty of calorimetric study under high-pressure environment, the present experimental technique is worth to be developed as a new method to determine heat capacity of mantle materials at high pressure and its pressure dependence.

### 3.4. Thermal conduction in the subducting slab

The thermal conductivity of garnet obtained in the present study has important implications for the thermal conduction through the mid ocean ridge basalt (MORB) layer in the subducting slab. MORB transforms to eclogite progressively below a depth of 100 km. In Table 5, thermal conductivity of basalt (Horai and Susaki, 1989) is compared with those of garnet (present study), diopside (Horai, 1971), and jadeite (Osako, in preparation). Eclogite is mostly composed of garnet and omphacitic pyroxene whose thermal conductivity is estimated from those of diopside and jadeite to be 4.8–6.8  $\text{W m}^{-1} \text{K}^{-1}$ . Therefore, the thermal conductivity of eclogite 3.5–6.8  $\text{W m}^{-1} \text{K}^{-1}$  should be at least three times larger than that of basalt at ambient conditions. The pressure dependence of thermal conductivity for

Table 4  
Heat capacity and its pressure derivative obtained in the present work

	Present results		Previous results	
	$C _{P=0}$ ( $\text{J kg}^{-1} \text{K}^{-1}$ )	$dC/dP$ ( $\text{J kg}^{-1} \text{K}^{-1} \text{GPa}^{-1}$ )	$C_P _{P=0}$ ( $\text{J kg}^{-1} \text{K}^{-1}$ )	$(\partial C_P/\partial P)_T$ ( $\text{J kg}^{-1} \text{K}^{-1} \text{GPa}^{-1}$ )
Garnet	711 (39)	1.6	706	−3.1
Olivine [1 0 0]	798 (42)	−1.5		
Olivine [0 1 0]	780 (60)	−3.4	816	−1.4
Olivine [0 0 1]	826 (40)	−5.3		

Heat capacity by Watanabe (1982) are also shown for comparison.  $(\partial C_P/\partial P)_T$  is calculated by substituting thermal expansivity data (Suzuki, 1975; Suzuki and Anderson, 1983) into a thermodynamic identity of  $((\partial C_P)/\partial P)_T = -T/\rho(\alpha^2 + (\partial\alpha)/(\partial T))_P$ .

Table 5  
Thermal conductivities ( $\lambda$ ) of basalt, jadeite, diopside, and garnet

	$\lambda$ ( $\text{W m}^{-1} \text{K}^{-1}$ )		$d\lambda/dP$ ( $\text{W m}^{-1} \text{K}^{-1} \text{GPa}^{-1}$ )	Reference
	293 K, 0 GPa	900 K, 3 GPa <sup>a</sup>		
Basalt	1.4	–	0.10	Horai and Susaki (1989)
Jadeite	6.8	2.5	0.31	Osako (in preparation)
Diopside	4.8	–	–	Horai (1971)
Garnet	3.5	4.9	0.15	This study

<sup>a</sup> Typical temperature and pressure condition for the basalt–eclogite phase transition boundary in the subducting slab.

basalt (Horai and Susaki, 1989), jadeite (Osako, in preparation) and garnet (this study) suggests that pressure enhances the difference. As a result unless  $d\lambda/dT$  of basalt is abnormally large, the eclogite layer of the slab transfer thermal energy much effectively from the hot mantle wedge (Furukawa, 1993) to warm the slab in contrast to the upper basaltic layer which may serve as a good thermal insulator.

#### 4. Concluding remarks

Thermal diffusivities and thermal conductivities of two major mantle minerals, garnet and olivine, were measured simultaneously by a pulse heating method under high pressure. Heat capacity was also obtained with the accuracy of 5%. Thermal conductivity of eclogite were estimated from the present result. Eclogite may be a thermal conductor in the subducting slab.

This method is useful for mantle materials because even small samples are feasible for measurement and anisotropy in thermal conduction can be determined. In the present measurements, the following step were made for improving the quality of data:

- (1) Maintain the boundary condition of constant temperature at the both sample end during the measurement.
- (2) Realize quasi-one dimensional heat flow in the sample.
- (3) Reduce noise by combining various techniques.

#### Acknowledgements

We thank T. Katsura for his help in the high-pressure experiment, and K. Yokoyama for EPMA analyses and helpful comments on the present samples. We

also thank anonymous reviewers for their helpful comments to improve the manuscript. This work was partly supported by a grant-in aid for Scientific Research (No. 14540401) from JSPS, and was carried out by joint research in the Institute for Study of the Earth's Interior, Okayama University.

#### References

- Beck, A.E., Darbha, D.M., Schloessin, H.H., 1978. Lattice conductivities of single-crystal and polycrystalline materials at mantle pressures and temperatures. *Phys. Earth Planet. Int.* 17, 35–53.
- Chai, M., Brown, J.M., Slutsky, L.J., 1996. Thermal diffusivity of mantle minerals. *Phys. Chem. Miner.* 23, 470–475.
- Cohen, R.E., 2000. MgO—The simplest oxide. In: Aoki, H., Syono, Y., Hemley, R.J. (Eds.), *Physics Meets Mineralogy*. Cambridge University Press, Cambridge, pp. 95–123.
- Dzhavadov, L.N., 1975. Measurement of thermophysical properties of dielectrics under pressure. *High Temp. High Pressures* 7, 49–54.
- Fujisawa, H., Fujii, N., Mizutani, H., Kanamori, H., Akimoto, S., 1968. Thermal diffusivity of  $\text{Mg}_2\text{SiO}_4$ ,  $\text{Fe}_2\text{SiO}_4$ , and NaCl at high pressures and temperatures. *J. Geophys. Res.* 73, 4727–4733.
- Furukawa, Y., 1993. Magmatic process under arcs and formation of the volcanic front. *J. Geophys. Res.* 98, 8309–8319.
- Hofmeister, A.M., 1999. Mantle values of thermal conductivity and the geotherm from phonon lifetimes. *Science* 283, 1699–1706.
- Horai, K., 1971. Thermal conductivity of rock-forming minerals. *J. Geophys. Res.* 76, 1278–1308.
- Horai, K., Susaki, J., 1989. The effect of pressure on the thermal conductivity of silicate rocks up to 12 kbar. *Phys. Earth Planet. Int.* 55, 292–305.
- Kanamori, H., Fujii, N., Mizutani, H., 1968. Thermal diffusivity measurement of rock-forming minerals from 300 to 1100 °K. *J. Geophys. Res.* 73, 595–605.
- Katsura, T., 1995. Thermal diffusivity of olivine under upper mantle conditions. *Geophys. J. Int.* 122, 63–69.
- Kobayashi, Y., 1974. Anisotropy of thermal diffusivity in olivine, pyroxene and dunite. *J. Phys. Earth* 22, 359–373.

- Manga, M., Jeanloz, R., 1997. Thermal conductivity of corundum and periclase and implications for the lower mantle. *J. Geophys. Res.* 102, 2999–3008.
- Osako, M., 1997. Thermal diffusivity of olivine and garnet single crystals. *Bul. Natl. Sci. Mus., Tokyo, Ser. E* 20, 1–7.
- Sato, Y., Akaogi, M., Akimoto, S., 1978. Hydrostatic compression of the synthetic garnets pyrope and almandine. *J. Geophys. Res.* 83, 335–338.
- Schärmeli, G.H., 1982. Anisotropy of olivine thermal conductivity at 2.5 GPa and up to 1500 K measured on optical non-thick samples. In: Schreyer, W. (Ed.), *High Pressure Researchs in Geoscience*. E. Schweizerbart'sche Verlagsbuchhandlung, Stuttgart, pp. 349–373.
- Suzuki, I., 1975. Thermal expansion of periclase and olivine and their anharmonic properties. *J. Phys. Earth* 23, 145–159.
- Suzuki, I., Anderson, O.L., 1983. Elasticity and thermal expansion of a natural garnet up to 1000 K. *J. Phys. Earth* 31, 125–138.
- Yukutake, H., Shimada, M., 1978. Thermal conductivity of NaCl, MgO, coesite and stishovite up to 40 kbar. *Phys. Earth Planet. Int.* 17, 193–200.
- Watanabe, H., 1982. Thermochemical properties of synthetic high-pressure compounds relevant to the Earth's mantle. In: Akimoto, S., Manghnani, M.H. (Eds.), *High Pressure Research in Geophysics*. Center for Academic Publication, Tokyo, pp. 441–464.
- Zha, C.S., Duffy, T.S., Downs, R.T., Mao, H.K., Hemley, R.J., 1998. Brilluin scattering and X-ray diffraction of San Carlos olivine: direct pressure determination to 32 GPa. *Earth Planet. Sci. Lett.* 159, 25–33.